Journal of Thermal Analysis and Calorimetry, Vol. 72 (2003) 1167–1174

POLYMER MELTING AND POLYMER POWDER SINTERING BY THERMAL ANALYSIS

A. Greco[*] *and A. Maffezzoli*

Department of Innovation Engineering, University of Lecce, Via Monteroni, 73100 Lecce, Italy

Abstract

Sintering of polymeric powders is a peculiar characteristic of many processing technologies, including rotational moulding and selective laser sintering (SLS). During polymer sintering, viscosity reduction in the melt state promotes densification of polymer powders, through a double stage mechanism, involving powder coalescence and bubble removal. In particular, sintering of semi-crystalline polymers is strongly influenced by the melting behaviour. Nevertheless, melting itself in absence of pressure is not necessarily accompanied by powder sintering, unless low viscosities are achieved. In this work, the melting and sintering behaviour of recycled high density polyethylene (rHDPE) have been analysed through differential scanning calorimetry (DSC) and Thermomechanical Analysis (TMA). Efficient models capable of describing the melting temperature distribution and rate of sintering of rHDPE powders have been developed, highlighting the inherent differences between the two distinct processes.

Keywords: melting, sintering, thermal analysis

Introduction

Melting and sintering of semi-crystalline polymeric materials are found in many industrial problems, where the lack of any pressure or force acting on the material requires low viscosities to allow surface tension forces overcoming viscous forces [1, 2]. The melting process of semi-crystalline polymers is usually observed in a broad temperature interval [3, 4]. The melting temperature of each crystal is mainly determined by its lamellar thickness [5]. Therefore the melting process depends on thermodynamic equilibrium, and is not significantly affected by kinetic effects. Sintering of polymers, defined as the formation of a homogeneous melt from coalescence of particles [2], is considered a double stage mechanism, involving powder coalescence [1, 2, 6] and bubble removal [7]. Surface area reduction (surface tension) is the driving force for sintering. Viscosity of polymer in the molten state plays a significant role since viscous forces must be overcome in order to allow powder coalescence [6]. Solid-state sintering is not possible for polymers, whereas the coalescence of particles begins only when certain conditions of mobility are achieved in the molten state [2]. Thus, although the two processes of melting and

---

[*] Author for correspondence: E-mail: antonio.greco@unile.it

1388–6150/2003/ $ 20.00

Akadémiai Kiadó, Budapest
Kluwer Academic Publishers, Dordrecht

sintering are strictly related, melting of polymers does not imply sintering of powders, unless adequately low viscosities are achieved. Too high viscosity in the molten state generates a high fraction of pores entrapped in the molten mass [7], and consequently poor quality products are obtained.

In this paper differential scanning calorimetry (DSC) has been used to analyse melting behaviour of recycled high density polyethylene, rHDPE. The melting process has been modelled using a statistical distribution function. Thermomechanical analysis (TMA) has been used to study sintering behaviour of rHDPE, and experimental data have been interpreted with a kinetic densification model. The differences between the two distinct processes have been highlighted.

Materials and methods

The material used is recycled HDPE originating from liquid containers, which has been shown to be a cost-effective raw material for rotational moulding, mixed with linear low density polyethylene [8]. Characterization of melting behaviour has been performed on a DSC 7 Perkin Elmer apparatus, heating samples from room temperature to 160°C at 10, 20, 30, 40 and 50°C min^{-1}. At each scanning rate the instrument has been calibrated through indium sample. Samples of the same size, weighing about 5 mg, have been tested in order to minimize thermal gradients within each sample. The signal has been elaborated to give the distribution of melting temperatures:

$$\frac{\mathrm{d}X_{\mathrm{m}}(T)}{\mathrm{d}T}=\frac{1}{H_{\mathrm{T}}}\frac{\mathrm{d}H(t)}{\mathrm{d}t}\frac{1}{\beta} \tag{1}$$

where $\mathrm{d}H(t)/\mathrm{d}t$ is DSC heat flow per unit mass, H_{T} is the total heat absorbed in the melting process, and $\beta=\mathrm{d}T/\mathrm{d}t$ is the scanning rate.

A Perkin Elmer thermomechanical analyser TMA 8 device has been used for the analysis of sintering process [9]. Samples of about 10 mg of HDPE powders, corresponding to an initial thickness of about 1 mm, have been tested. Heating scans have been run between 40 and 200°C at 3, 5 and 10°C min^{-1}. At each scanning rate the instrument has been calibrated through indium sample. The pressure on the sample has been kept very low (35 Pa) in order to better simulate the zero-pressure sintering process occurring during rotational molding. The average diameter of HDPE powders, determined from optical microscopy, is 0.41 mm. The size distribution of powders is reported in Table 1. The advancement of sintering has been evaluated from the ratio between the sample thickness at the beginning of the test L_{i} and the thickness at time t, $L(t)$. Each set of TMA experimental data is obtained as the average of three tests.

Table 1 Powder diameter distribution determined from optical microscopy

Diameter/mm	0.235	0.305	0.375	0.445	0.515	0.585
Number fraction	0.05128	0.07692	0.33333	0.4359	0.07692	0.02564

Results and discussion

Melting of polyethylene

It is generally accepted that the DSC melting peak can be regarded as a distribution of melting temperatures of crystallites, resulting from a distribution of lamellar thickness [3, 4, 10]. Consequently the integral curve of the DSC melting peak, defined as the degree of melting X_m, is regarded as the cumulative distribution curve. Therefore the melting temperature distribution can be modelled, following a statistical approach, as the derivative of a sigmoidal growth curve [11] such as the SRichards function [12]:

$$\frac{dX_m}{dT}(T)=k_m(\exp(-k_m(T-T_p)))(1+(d-1)\exp(-k_m(T-T_p)))^{d/(1-d)} \tag{2}$$

where T_p is the temperature corresponding to the peak of the signal, that is regarded as the most probable melting temperature, k_m is an intensity factor, and d is the shape factor. Equation (2) is a two-parameter fitting equation, since T_p can be determined from experimental data. An increase of k_m results in increasing the peak value and in a lower dispersion around the most probable value, whereas increasing d results in a higher dispersion of melting temperatures at lower values than the most probable one. In Fig. 1 DSC curves obtained at different heating rates are reported. In Fig. 1 no superheating effect [5], or annealing effect, involving an exothermic peak [10], can be observed. The shape of the curves of Fig. 1 is essentially the same for every scanning rate, and the temperature shift (peak temperature in Table 2) is attributed to thermal lag effects in the DSC oven [4, 13]. On the other hand, the melting enthalpy does not depend on the heating rate, as shown in Table 2. Following the procedure proposed by Zhou and Wilkes [4], the actual distribution is obtained by linear extrapolation of experimental melting peaks at zero heating rate. The curves are then shifted to the new position corresponding to T_p=402.3 K. No attempt is made to correct the shape of the distribution, since its relation to the heating rate is complex [4, 13], and

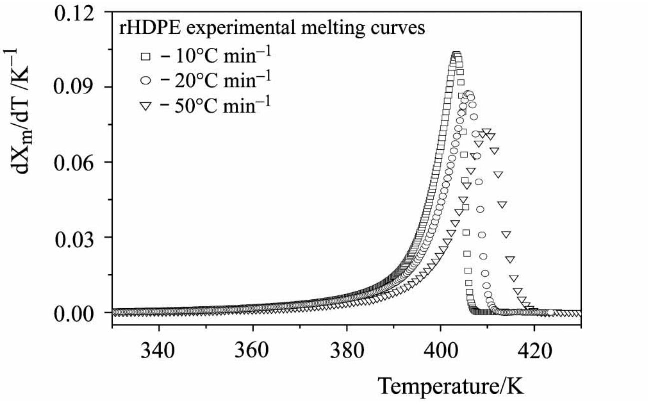

Fig. 1 Experimental data of melting temperature distribution dX_m/dT for rHDPE melting at □ – 10, ○ – 20 and ▽ – 50°C min^{-1}

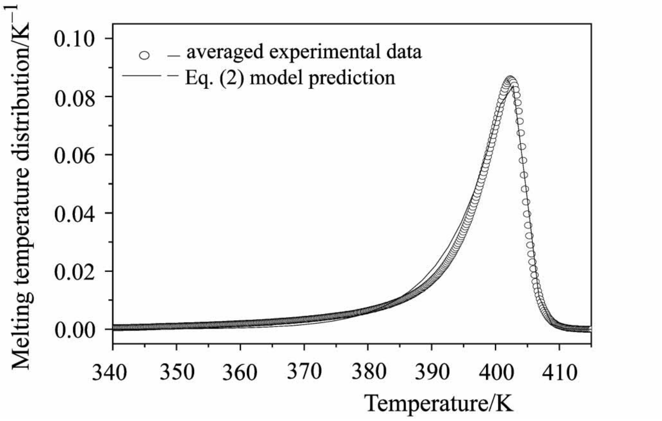

Fig. 2 Averaged ○ – experimental data and —— – model prediction according to Eq. (2)

the curves are characterized by similar shapes after extrapolation procedure. The average of extrapolated curves, reported in Fig. 2, has been fitted according to the statistical models of Eq. (2). Good agreement between experimental data and model prediction is observed in Fig. 2. The numerical values for the parameter of Eq. (2) are reported in Table 3.

Table 2 Melting enthalpy and peak temperature for rHDPE determined from DSC experiments at different scanning rates

Scanning rate/°C min^{-1}	Melting enthalpy/J g^{-1}	Peak temperature/K
10	170.64	403.354
20	170.23	405.820
30	166.89	407.258
40	164.17	408.154
50	167.52	409.820

Table 3 Numerical values of fitting parameters for Eqs (2) and (3)

k_m/K^{-1}	0.96503
d	8.58414
k_0/s^{-1}	$1.3\cdot10^6$
E/R /K	730

Sintering behaviour of polyethylene powders

TMA experiments have been performed on HDPE powders. The bulk density of powders is determined as the ratio between their mass and apparent volume, and is reported in Table 4. In Fig. 3 the rate of sintering, defined as the derivative of TMA out-

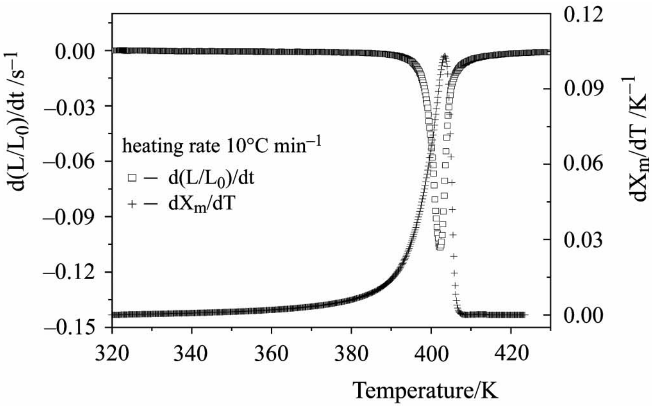

Fig. 3 Comparison between rate of □ – sintering d(L/L_0)/dt and + – melting temperature distribution dX_m/dT for rHDPE

put, d(L/L_0)/dt, is compared with the melting endotherm obtained from DSC analysis. Sintering does not take place until sample temperature exceeds the initial melting temperature. This has been previously observed for semi-crystalline polymers [2], and is mainly due to the need of a finite viscosity to allow sintering process, as predicted by the Frenkel model [6]. Then the sintering rate suddenly increases as a consequence of high initial void fraction and viscosity reduction, and reaches its maximum at a temperature (402.29 K) only slightly lower than the DSC melting peak temperature (403.35 K), which is mainly determined by the lamellar thickness distribution of crystals. After melting has completed, at about 407.5 K, sintering continues, according to the kinetic model derived by Kandis *et al.* [1], and modified, as in Eq. (3), to take into account for the zero rate of sintering in the solid state:

$$\frac{d\chi(t)}{dt}=-k_0\exp\left(-\frac{E}{R(T-T_{on})}\right)(\chi(t)-\chi_\infty) \tag{3}$$

$$\chi(t)=1-\frac{\rho(t)}{\rho_0} \tag{4}$$

$$\rho(t)=\rho_i\frac{L(t)}{L_i} \tag{5}$$

where χ is the void fraction, T_{on} is the onset temperature for melting, χ_∞ is the final void fraction, E is the activation energy for the sintering process, k_0 is the kinetic constant, ρ is the apparent density, ρ_i is the initial bulk density of powders and ρ_0 is the density of HDPE, taken as 950 kg m^{-3}. L_i is the initial thickness of TMA samples, and $L(t)$ is the sample thickness as measured by TMA. Density and linear shrinkage are simply correlated by Eq. (5) assuming that no shrinkage occurs in the plane perpendicular to the sample thickness. The final void fraction χ_∞ has been determined by optical microscopy of sintered samples, and is reported in Table 4, together with the initial density (bulk den-

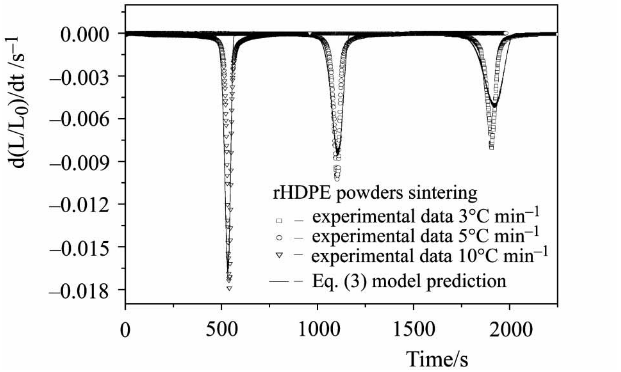

Fig. 4 Experimental data for rHDPE rate of sintering d(L/L_0)/dt at □ – 3, ○ – 5 and ▽ – 10°C min^{-1}, and model prediction according to Eq. (3)

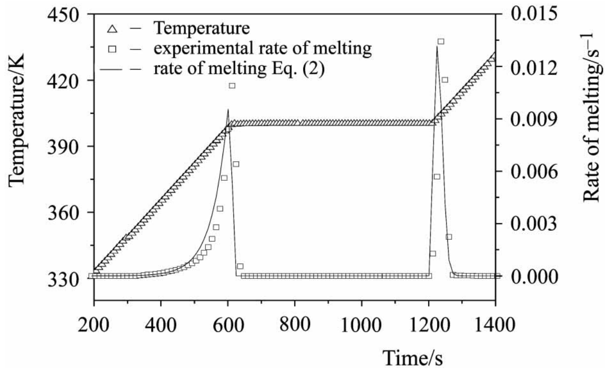

Fig. 5 Temperature history with isothermal step in the melting range of △ – rHDPE, experimental rate of □ – melting dX_m/dT and model prediction according to Eq. (2)

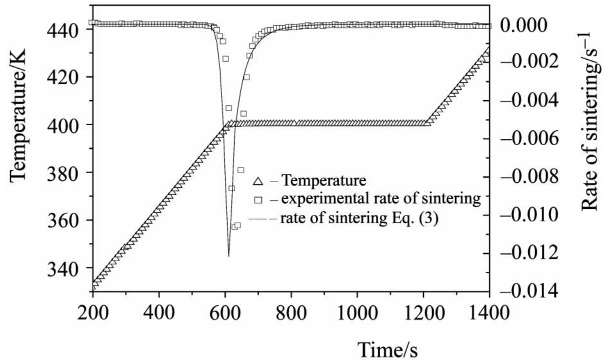

Fig. 6 Temperature history with isothermal step in the melting range of △ – rHDPE experimental rate of □ – sintering d(L/L_0)/dt for the temperature program, and model predictions according to —– Eq. (3)

sity) ρ_i. The numerical value of the parameters E and K_0 have been determined by non linear regression of experimental data. The predictions according to the model of Eqs (3)–(5) are compared with experimental data at different heating rates in Fig. 4 for HDPE powders. Good agreement is observed between experimental data and model prediction. Further, in Fig. 5, a comparison between experimental melting behaviour of HDPE and model prediction according to Eq. (2) is shown, when a complex thermal history is applied. Both experimental and model curves are obtained using the following thermal history: 1) heating scan at 10°C min^{-1}; 2) isothermal step at 127°C, where melting has begun, but not yet completed; 3) further heating at 10°C min^{-1} up to 160°C to complete melting. In Fig. 6 the comparison between experimental sintering behaviour and model prediction according to Eqs (3)–(5) is shown, when the same thermal history is applied. The DSC experimental curve of Fig. 5 indicates that no melting takes place during the isothermal step at 127°C, which is consistent with the assumption of a statistical distribution of melting temperature. Melting can continue only when temperature is raised again to higher temperatures. The overall melting behaviour of the material reported in Fig. 5 is well predicted by the statistical model of Eq. (2). On the other hand, the sintering behaviour is much different: once sintering has begun, it continues also during the isothermal step at 127°C. Once the temperature is raised again, sintering of the sample has already been completed, and no further shrinkage of the sample is observed. The sintering behaviour of rHDPE is well described by the kinetic model applied, Eq. (3), which predicts a non-zero rate of sintering during isothermal step.

Table 4 Initial and final conditions for integration of Eq. (3) as determined from experimental data

Powders bulk density/kg m^{-3}, ρ_i	347.1±5.56
Void fraction after sintering, χ_∞	0.02375

Conclusions

In this work differential scanning calorimetry and thermomechanical analysis have been used to study melting and sintering behaviour of recycled high density polyethylene rHDPE. The DSC melting peak, regarded as a statistical distribution of lamellar crystal thicknesses, has been successfully modelled using a properly developed distribution function. Experimental data well agrees with the statistical model showing the presence of unmolten crystals when the temperature is kept constant in the melting range. Only further heating leads to complete melting both in experimental DSC data and in the statistical model predictions. The presented statistical approach can be a valuable tool for modelling heat transfer phenomena occurring in rotational molding. On the other hand, sintering behaviour of rHDPE has been modelled using a kinetic model derived from Frenkel's equation for viscous sintering. A comparison between the two processes during isothermal staying in the melting range of rHDPE shows that the two processes, though strictly correlated, are well distinct, and governed by different mechanisms, namely the distribution of lamellar thickness for melting and viscosity reduction for sintering.

References

1 M. Kandis and T. L. Bergman, J. Heat Transfer, 119 (1997) 824.
2 S. J. Liu, Int. Polymer Proc. XIII, Hanser Publishers, Munich 1998, pp. 88–90.
3 L. Lu, R. G. Alamo and L. Mandelkern, Macromolecules, 27 (1994) 6571.
4 H. Zhou and G. L. Wilkes, Polymer, 38 (1997) 5735.
5 E. Hellmuth and B. Wunderlich, J. Appl. Physics, 36 (1965) 3039.
6 C. T. Bellehumeur, M. K. Bisaria and J. Vlachopoulos, Polymer Eng. Sci., 36 (1996) 2198.
7 M. Kontopoulou and J. Vlachopoulos, Polymer Eng. Sci., 39 (1999) 1189.
8 A. Greco, M. Frigione and A. Maffezzoli, Polymer Recycling, 6 (2001) 23.
9 R. S. Nasar, M. Cerqueira, E. Longo and J. A. Varala, Ceramics Int., 25 (1999) 593.
10 M. E. Nichols and R. E. Robertson, J. Polymer Sci.: Part B: Polymer Physics, 30 (1992) 755.
11 J. A. Drakopoulos, Fuzzy Sets and Systems, 99 (1998) 57.
12 G. A. F. Seber and C. J. Wild, Nonlinear Regression, John Wiley & Sons, New York 1989, pp. 332–337.
13 J. G. Plummer and H. H. Kausch, Polymer Bulletin, 36 (1996) 355.